

Study of Proton- $^{9,11}\text{Li}$ Elastic Scattering at 60~75 MeV/Nucleon

Arafa A. Alholaisi, Jamal H. Madani, M. A. Alvi

Abstract—The radial form of nuclear matter distribution, charge and the shape of nuclei are essential properties of nuclei, and hence, are of great attention for several areas of research in nuclear physics. More than last three decades have witnessed a range of experimental means employing leptonic probes (such as muons, electrons etc.) for exploring nuclear charge distributions, whereas the hadronic probes (for example alpha particles, protons, etc.) have been used to investigate the nuclear matter distributions. In this paper, p - $^{9,11}\text{Li}$ elastic scattering differential cross sections in the energy range 60 to 75 MeV have been studied by means of Coulomb modified Glauber scattering formalism. By applying the semi-phenomenological Bhagwat-Gambhir-Patil [BGP] nuclear density for loosely bound neutron rich ^{11}Li nucleus, the estimated matter radius is found to be 3.446 fm which is quite large as compared to so known experimental value 3.12 fm. The results of microscopic optical model based calculation by applying Bethe-Brueckner-Hartree-Fock formalism (BHF) have also been compared. It should be noted that in most of phenomenological density model used to reproduce the p - ^{11}Li differential elastic scattering cross sections data, the calculated matter radius lies between 2.964 and 3.55 fm. The calculated results with phenomenological BGP model density and with nucleon density calculated in the relativistic mean-field (RMF) reproduces p - ^9Li and p - ^{11}Li experimental data quite nicely as compared to Gaussian-Gaussian or Gaussian-Oscillator densities at all energies under consideration. In the approach described here, no free/adjustable parameter has been employed to reproduce the elastic scattering data as against the well-known optical model based studies that involve at least four to six adjustable parameters to match the experimental data. Calculated reaction cross sections σ_R for p - ^{11}Li at these energies are quite large as compared to estimated values reported by earlier works though so far no experimental studies have been performed to measure it.

Keywords—Bhagwat-Gambhir-Patil density, coulomb modified Glauber model, halo nucleus, optical limit approximation.

I. INTRODUCTION

LAST several decades have witnessed a variety of experimental methods using leptonic probes (such as muons, electrons, etc.) for exploring nuclear charge distributions whereas the hadronic probes (for example protons, alpha particles, etc.) are used for investigating the distributions of nuclear matter. While all these approaches were fruitfully employed for several years to study the stable nuclei, the examination of the shape and radial extent of exotic nuclei has developed a fresh and exhilarating field of research [1], [2]. The nuclei located at far away from the stability line in nuclear chart called exotic nuclei. These exotic nuclei are unstable, and their lifetimes vary from a milli second to a

second, which are much longer than the time scale of nucleonic motion ($\sim 10^{-23}$ s) inside the nucleus. Since, these nuclei short lived and rapidly decayed, they can be produced by nuclear reaction with radioactive ion beam in inverse kinematics.

The method of elastic proton-nucleus scattering in the energy range 700~1000 MeV is well established for finding precise and thorough knowledge on the radial shape and size of exotic nuclear matter distributions [3]. Differential cross sections for elastic scattering of proton with neutron-rich lithium nuclei ^8Li , ^9Li and ^{11}Li (likely having halo structure) for small-angle scattering were experimentally carried out at energy nearby 700 MeV/nucleon, and experimental data were analyzed by means of Glauber scattering theory [4], [5]. Using GG (Gaussian-Gaussian) and GO (Gaussian-oscillator) parameterization for modelling the nucleon distribution in Li nucleus, calculation of Egelhofaf [4] indicates nuclear matter radius of ^{11}Li to be 3.53 fm, quite large compared to that of ^{11}Li ($3.12 \pm 0.16\text{fm}$) by Tanihata et al. [1], [2]. Moreover, in a similar approach, Dobrovolsky et al. [5] suggests a slightly less stretched matter distribution with a value $3.42 \pm 0.11\text{fm}$ for ^{11}Li . It is to be noted that in above these two theoretical analyzes of $^{9,11}\text{Li}$ at proton beam energy about 700 MeV, two free nuclear density parameters are used in least square fitting to reproduce the experimental data. Further, slightly more advanced method [6] that takes into account three-body character, suggests $3.55 \pm 0.10\text{fm}$. for rms matter density radius of ^{11}Li , which is similar to that obtained by Egelhofaf [4].

Elastic p - $^{9,11}\text{Li}$ scattering angular distributions data are available in the energy range 60~75 MeV [7]. Most of the theoretical studies of elastic scattering of p - $^{6,7,9,11}\text{Li}$ at energy range 40~75 MeV are based on optical model as for example, Hassan et al. [8] calculated the real part of the potential, using folding technique and effective NN force, whereas the imaginary part is acquired with Woods-Saxon shape in analyzing the elastic p - ^{11}Li scattering cross sections. The microscopic optical potential has been utilized to calculate scattering cross section for p - ^{11}Li at energies 62,68.4 and 75 MeV in [9]. The folding approach and the density-dependent M3Y effective interactions are employed to evaluate the real part of optical potential and the imaginary part is considered microscopically inside the folding model. For ^{11}Li nuclear density, the LSSM densities [9] have been used for protons and neutrons. In the framework of microscopic optical potential, hybrid model [10] is applied to study the differential elastic scattering cross sections for p - ^{11}Li and the total cross sections for reaction at energies 62,68.4, and 75 MeV. Very

Arafa A. Alholaisi is with the King Abdulaziz University, Saudi Arabia (e-mail: arafa1408@gmail.com)

recently, Sharma and Haider [11] by applying BHF formalism, have analyzed the elastic scattering differential cross section data for p - ^{11}Li at energy range 62~75 MeV by considering microscopic optical potential.

In this work, p - ^9Li and p - ^{11}Li elastic scattering differential cross section in the energy range 60~75 MeV have been analyzed by means of Coulomb modified Glauber scattering formalism [12]. By applying the semi-phenomenological BGP [13] nuclear density for loosely bound nuclei, the information on the nuclear matter distributions has been extracted. In addition, GG and GO [5] nuclear density models have also been used in the analysis of p - ^{11}Li elastic scattering experimental data. The *rms* matter density and total reaction cross sections σ_R are compared with results obtained by earlier researchers.

II. EVOLUTION OF ELASTIC P-NUCLEUS DIFFERENTIAL CROSS SECTION

A. Glauber Formalism

In the Glauber multiple scattering formalism [14], the amplitude for the elastic scattering of a projectile nucleon with a target nucleus, mass number A described by the ground state wave function Ψ_0 may be expressed as:

$$F_{el}(\mathbf{q}) = \frac{iK}{2\pi} \int d\mathbf{b} e^{i\mathbf{q}\cdot\mathbf{b}} (1 - S_{el}(b)) \quad (1)$$

where K is the *c.m.* momentum of the projectile-nucleus system and $S_{el}(b)$ in the impact parameter space \mathbf{b} , represents the elastic scattering S -matrix element which is connected to the optical phase shift-function $\chi(b)$ as:

$$S_{el}(b) = e^{i\chi(b)} = \langle \Psi_0 | \prod_{i=1}^A [1 - \Gamma_{NN}(b - s_j)] | \Psi_0 \rangle \quad (2)$$

where $\Gamma_{NN}(b)$ is the nucleon-nucleon (NN profile function and s_i is the two-dimensional coordinate of the i -th target nucleon relative to its center of mass that lies on the plane perpendicular to projectile momentum. The profile function $\Gamma_{NN}(b)$ is the Fourier transform of NN scattering amplitude $f_{NN}(q)$:

$$\Gamma_{NN}(b) = \frac{1}{2\pi i k} \int e^{-i\mathbf{q}\cdot\mathbf{b}} f_{NN}(q) dq \quad (3)$$

Applying so called the optical limit approximation (OLA) and utilizing the normalized intrinsic density $\rho(r)$ for the target nucleus, (2) reduces to:

$$e^{i\chi(b)} = \exp[-A \int dr \Gamma_{NN}(b - s) \rho(r)]. \quad (4)$$

where, k represents the projectile nucleon momentum. The Glauber model multiple scattering theory is very successful for the small angle high energy scattering and the Gaussian parameterization of $f_{NN}(q)$ has effectively been applied in explaining the elastic scattering differential cross section experiments [12], [15], [16]. To apply this model to some lower energies such as below 100 MeV, its helpfulness should be handled cautiously. Therefore, we treat the interactions of

proton-proton and proton-neutron separately and write $f_{NN}(q)$ as:

$$f_{pi}(q) = \frac{ik\sigma_{pi}}{4\pi} (1 - i\alpha_{pi}) e^{-\beta_{pi}q^2/2}, i = p(n) \quad (5)$$

where, the parameter $\beta_{pp}(\beta_{pn})$ are pp (pn) slope parameters of elastic scattering differential cross section and $\sigma_{pp}(\sigma_{pn})$ and $\alpha_{pp}(\alpha_{pn})$ are respectively, the total cross section and the ratio of the real to imaginary parts of the forward scattering amplitude. Using (5), (4) can be written as:

$$S_{el}(b) = e^{i\chi(b)} = \exp\left[\frac{iZ}{k} \int_0^\infty q dq J_0(qb) f_{pp}(q) F_p(q) + \frac{i(A-Z)}{k} \int_0^\infty q dq J_0(qb) f_{pn}(q) F_n(q)\right] \quad (6)$$

Substituted (6) in (1) the elastic scattering amplitude $F_{el}(q)$ can easily be calculated.

To account the deviation of projectile trajectory due to Coulomb field, one replaces impact parameter b in the elastic S -matrix element $S_{el}(b)$ by the distance of closest approach b' [12]. The distance of closest approach is associated to b as:

$$b' = \xi + \sqrt{(\xi)^2 + b^2} \quad (7)$$

with, $\xi = \eta/K$ where K is the *c.m.* momentum of the projectile-nucleus system as before, $\eta = \frac{Ze^2}{\hbar v}$ denotes the Sommerfeld parameter and v the incident nucleon velocity. The final expression for elastic scattering differential cross sections for p -nucleus may be calculated by:

$$\frac{d\sigma}{d\Omega} = |F_c(q) + F_{el}(q)|^2 \quad (8)$$

where $F_c(q)$ is the usual point Coulomb scattering amplitude.

B. Parameters of NN Amplitude $f_{NN}(q)$

The parameters σ_{pp} and σ_{pn} of NN amplitude have been obtained by using the formula in [12] which in the energy range 101000 MeV reproduce observed values nicely:

$$\sigma_{pp} = 13.73 - 15.04v^{-1} + 8.7v^{-2} + 68.67v^4 \quad (9)$$

$$\sigma_{pn} = -70.67 - 18.18v^{-1} + 25.26v^{-2} + 113.85v \quad (10)$$

where, σ_{pp} and σ_{pn} are defined in mb while to calculate parameters α_{pp} and α_{pn} we use Ahmad et al. [17] parameterization:

$$\alpha_{pp} = -0.386 + 1.224 \exp\left[-0.5 \left(\frac{k-0.427}{0.178}\right)^2\right] + 1.01 \exp\left[-0.5 \left(\frac{k-0.592}{0.638}\right)^2\right] \quad (11)$$

$$\alpha_{pn} = -0.666 + 1.437 \exp\left[-0.5 \left(\frac{k-0.412}{0.196}\right)^2\right] + 0.617 \exp\left[-0.5 \left(\frac{k-0.797}{0.291}\right)^2\right], \quad (12)$$

with incident nucleon lab momentum k is given in GeV/c.

The evaluated parameter values of $f_{NN}(q)$ at these energies are quoted in Table I. It is to be noted that values of β_{pp} (β_{pn}) are taken from [16] but at 68.4 and 75 MeV are with average of these quantities between energies 60 and 80 MeV and then between 70 and 80 MeV, respectively.

III. PARAMETERIZATIONS OF THE DENSITY DISTRIBUTIONS OF NUCLEUS

In this work, the halo nuclei ${}^9\text{Li}$ and ${}^{11}\text{Li}$ are considered to have two valence nucleons. More specifically, in this picture, the neutron densities of ${}^9,{}^{11}\text{Li}$ are expressed as:

$$\rho_n({}^9\text{Li}; r) = \rho_n(N=4; Z=3; r) + \rho_n(N=2; r),$$

$$\rho_n({}^{11}\text{Li}; r) = \rho_n({}^9\text{Li}; r) + \rho_n(2; r)$$

A. Gambhir and Patil (GP) Density

The Gambhir and Patil (GP) phenomenological nuclear density [18] $\rho_{n(p)}(r)$ is demonstrated by following formula:

$$\rho_i(r) = \frac{\rho_i^0}{1 + \left[0.5 \left(1 + \frac{r^2}{R^2}\right)\right]^{\alpha_i} \left(e^{\frac{(r-R)}{\alpha_i}} + e^{-\frac{(r+R)}{\alpha_i}} \right)}; \quad i = p, n \quad (14)$$

with

$$\alpha_i = \frac{\hbar}{2\sqrt{2m\epsilon_i}} \quad \text{and} \quad \alpha_i = \frac{q}{\hbar} \sqrt{\frac{m}{2\epsilon_i}} + 1 \quad (15)$$

where ϵ_i stands for the separation energy of the outermost proton or neutron, m is the nucleon mass, and

$$q = \begin{cases} (z-1)e^2 & \text{proton} \\ 0 & \text{neutron.} \end{cases}$$

The two unknown entities ρ_p^0, ρ_n^0 are the normalization constant of the proton and neutron densities. Thus, parameter R called half density radius is calculated by putting the experimental charge root mean square radius (r_{msr}) r_c of the nucleus same as obtained by GP model proton density r_{msr} r_p after accounting for the charge r_{msr} of a proton.

For neutron-rich nuclei, the phenomenological nuclear GP [18] density is modified by BGP [13] and the total neutron density is assumed to be composed of core and tail parts:

$$\rho_n(r) = \rho_n^{core}(r) + \rho_n^{tail}(r) \quad (16)$$

where, the core part $\rho_n^{core}(r)$ is given by (14) and the tail part $\rho_n^{tail}(r)$ of the halo nuclei takes the form:

$$\rho_n^{tail}(r) = N_0 \left[\frac{r^2}{(r^2 + R^2)^2} \right] \left(e^{\frac{r}{a_t}} + e^{-\frac{r}{a_t}} \right)^{-1} \quad (17)$$

with, $a_t = \frac{\hbar}{2\sqrt{2m\epsilon_t}}$. Here, ϵ_t indicates the separation energy of neutron of the halo nucleus with total neutron number N , whereas, R in the tail part corresponds to the core nucleus with

proton number Z and neutron number $N_c = N - N_t$, where N_t is the number of neutrons in the tail. The normalization constant N_0 is determined by requiring that $\rho_n^{tail}(r)$ should give the exact neutrons number in the tail (halo). It is to point out that (17) has the expected feature. Its asymptotic behavior as seen from (17) is peaked near the surface region while vanishing out at the center.

The proton density (N, Z) is calculated from the (14) by taking separation energy of proton ϵ_p and R corresponding to the nucleus (N, Z). By this, one expects that the slight difference in the distribution of proton within the core (N_c, Z) and the lightly bound nucleus (N, Z) has been taken into account at least approximately.

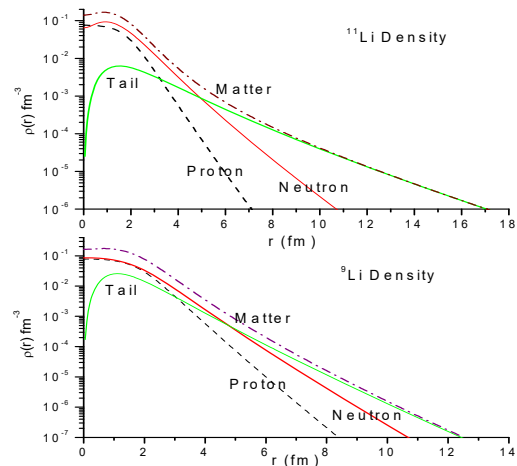


Fig. 1 Proton, neutron, tail and matter density distributions in ${}^9\text{Li}$ and ${}^{11}\text{Li}$ deduced using BGP phenomenological model

B. GG Density

The GG [8] phenomenological density distributions assume that the nuclei consist of (core + tail) nucleons with different spatial Gaussian distributions:

$$\rho_i(r) = \left[\frac{3}{2\pi R_i^2} \right]^{\frac{3}{2}} \exp\left(\frac{-3r^2}{2R_i^2} \right) \quad (18)$$

where $i = c, t$ denotes the core R_c and tail R_t and are the r_{ms} radii of the core and tail nucleon distributions $\rho_c(r)$ and $\rho_t(r)$, respectively.

C. GO Density

The GO [8] density distributions in the halo nuclei, the core is same as a Gaussian given by (18) whereas the tail density $\rho_t(r)$ is $1p$ -shell harmonic oscillator distribution which are expressed as:

$$\rho_t(r) = \frac{5}{3} \left[\frac{5}{2\pi R_t^2} \right]^{\frac{3}{2}} \left(\frac{r^2}{R_t^2} \right) \exp\left(\frac{-5r^2}{2R_t^2} \right) \quad (19)$$

The total matter density distribution $\rho_m(r)$, normalized to

unity and the matter radius R_m in both the GG and GO densities are expressed as:

$$\rho_m(r) = [N_c \rho_c(r) + (A - N_c) \rho_t(r)] / A \quad (20)$$

$$R_m = \left[\frac{N_c R_c^2 + (A - N_c) R_h^2}{A} \right]^{1/2} \quad (21)$$

where N_c and A indicate respectively, the nucleons number in the core and the nuclear mass number.

TABLE I
PARAMETER VALUES OF THE NN ELASTIC SCATTERING AMPLITUDE AT SEVERAL ENERGIES

| E(MeV) | $\sigma_{pp}(fm^{-2})$ | α_{pp} | $\beta_{pp}(fm^{-2})$ | $\sigma_{pn}(fm^{-2})$ | α_{pn} | $\beta_{pn}(fm^{-2})$ |
|--------|------------------------|---------------|-----------------------|------------------------|---------------|-----------------------|
| 60 | 4.575 | 1.637 | 0.335 | 13.16 | 0.86 | 0.455 |
| 62 | 4.375 | 1.657 | 0.335 | 12.66 | 0.88 | 0.455 |
| 68.4 | 3.990 | 1.710 | 0.310 | 11.36 | 0.93 | 0.413 |
| 75 | 3.632 | 1.758 | 0.297 | 10.14 | 0.98 | 0.393 |

IV. RESULTS AND DISCUSSION

We, first present and discuss here the result of phenomenological density distributions evaluated by BGP [13] for ${}^9\text{Li}$ and ${}^{11}\text{Li}$ nuclei and compare *rms* radii with reported earlier studies. For ${}^9\text{Li}$, we have found the *rms* matter radius to be $2.56 fm$ as compared to so called experimental value $2.61 fm$ obtained by Tanihata et al. [2]. Using four different phenomenological model density distribution for ${}^9\text{Li}$, Dobrovolsky et al. [5] indicated it to be $2.44 \pm 0.06 fm$ which is further smaller than that of [1]. The radial shape of nuclear matter distribution in ${}^9\text{Li}$ has been demonstrated in Fig. 1.

In Table II, we have presented the results of calculated matter, proton, neutron, core and halo (tail) radii using semi-phenomenological BGP model density distribution for ${}^{11}\text{Li}$. For comparison, corresponding radii obtained stated earlier have also been displayed in the same Table. It is clear that *rms* radius of ${}^{11}\text{Li}$ is significantly larger than that of ${}^9\text{Li}$. The ${}^{11}\text{Li}$, known as a Borromean nucleus [19], which is a three-body structure of nucleons that spaced out if any one of them is removed. It is also seen that the calculated core size of ${}^{11}\text{Li}$ is larger than the experimentally obtained radius of ${}^9\text{Li}$, which has been considered as the core in ${}^{11}\text{Li}$. The reason for upsurge in core size may be due to the movement of center of mass of core about the center of mass of the entire nucleus.

It is to be noted that calculated matter radius varies with minimum $2.964 fm$ by Karataglidis et al. [20] to a maximum $3.55 fm$ obtained by Al-Khalili and Tostevin [6] and with GG model density distribution by Dobrovosky et al. [5]. It is seen from Table II that in most of phenomenological density model used to reproduce the $p-{}^{11}\text{Li}$ differential elastic scattering cross sections, obtained matter radius is quite large as compared to so known experimental value $3.12 fm$ by Tanihata et al. [1]. Interestingly, similar pattern also seen for tail (halo) radius however, not large variations are found in the value of *rms* core radius obtained by various calculations reported in this work. In Fig. 1, we have also demonstrated the radial shape of nuclear matter distribution in ${}^{11}\text{Li}$.

Finally, we present and discuss the results of $p-{}^9-{}^{11}\text{Li}$ elastic differential cross sections $\frac{d\sigma}{d\Omega}$ in the incident energies range $60-75 MeV$ using the Coulomb modified Glauber model [12]. The experimental data have been taken from [7]. Fig. 2 displays the $p-{}^9\text{Li}$ elastic scattering at $60 MeV$ where the black solid line represents the result with BGP density and circles represent the experimental data. It is seen that our calculations using BGP proton and neutron density distribution reproduces the experimental data over the whole angular range. For comparison, we also performed calculation using GG and GO density [5] and both these density distribution, yield almost identical results and is difficult to identify the plotted curves in the figure, which are represented by olive dash-dotted curve. It is seen that calculated results with GG or GO density distribution does not reproduce experimental data beyond 45° .

TABLE II
THE CALCULATED RMS PROTON (r_p), NEUTRON (r_n), MATTER (r_{matter}), CORE (r_{core}), AND HALO) RADII FOR ${}^{11}\text{Li}$

| Authors | (fm) | | | | |
|-------------------------------------|--------|-------|--------------|------------|------------|
| | r_p | r_n | r_{matter} | r_{core} | r_{halo} |
| Present calculation | 2.17 | 3.82 | 3.446 | 2.85 | 5.37 |
| Tanihata et al [1] | | 3.21 | 3.12 | 2.61 | 4.8 |
| Egelhofaf [4] | | | 3.53 | 2.54 | 6.28 |
| ${}^{11}\text{Li}$ Rafi et al. [21] | 2.334 | 3.677 | 3.364 | | |
| Karataglidis et al. [20] | | | 2.964 | | |
| AlKhalili and Tostevin [9] | | | 3.55 | | |
| Dobrovosky et al. [5] | | | 3.55 | 2.56 | 6.31 |
| | | | 3.37 | 2.50 | 5.86 |

For comparison, the corresponding radii found stated previously have also been indicated.

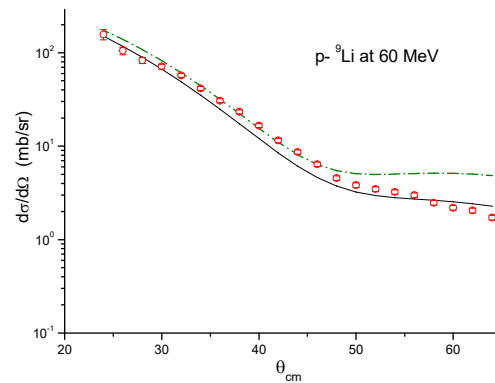


Fig. 2 The calculated differential cross section for $p-{}^9\text{Li}$ scattering at $60 MeV$; black solid line is obtained by using semi-phenomenological BGP nucleon density distributions and green olive dash-dotted line with GO density [5]. The data in circles are taken from [7]

Finally, we present and discuss the results of $p-{}^9-{}^{11}\text{Li}$ elastic differential cross sections $\frac{d\sigma}{d\Omega}$ in the incident energies range $60-75 MeV$ using the Coulomb modified Glauber model [12]. The experimental data have been taken from [7]. Fig. 2 displays the $p-{}^9\text{Li}$ elastic scattering at $60 MeV$ where the black solid line represents the result with BGP density and

circles represent the experimental data. It is seen that our calculations using BGP proton and neutron density distribution reproduces the experimental data over the whole angular range. For comparison, we also performed calculation using GG and GO density [5] and both these density distribution, yield almost identical results and is difficult to identify the plotted curves in the figure, which are represented by olive dash-dotted curve. It is seen that calculated results with GG or GO density distribution does not reproduce experimental data beyond 45° .

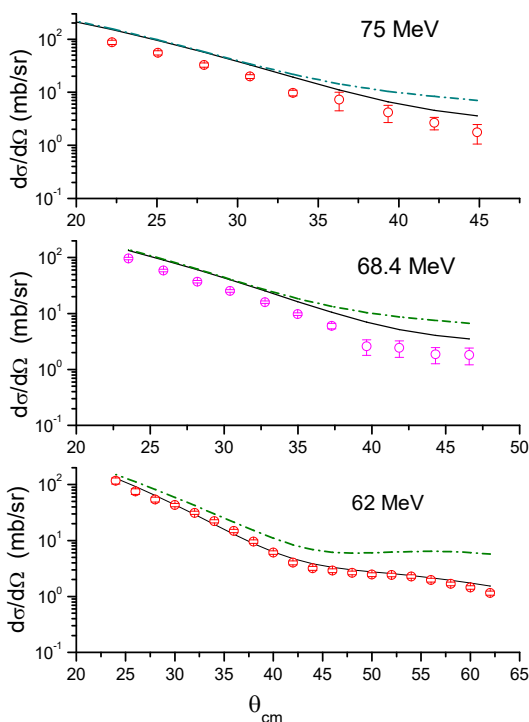


Fig. 3 The calculated differential cross section for $p-^{11}\text{Li}$ scattering at 62,68.4 and 75 MeV; Black solid line is obtained by using semi-phenomenological BGP nucleon density distributions and green olive dash-dotted line with GO density [5]. The data in circles are taken from [7]

The calculated differential cross sections in the case of $p-^{11}\text{Li}$ at energies 62,68.4 and 75 MeV are shown in Fig. 3. It is obvious from the figure that results with BGP model density reproduces experimental data fairly well as compared to GG or GO densities [5] at all energies under consideration. In fact, for $p-^{11}\text{Li}$ at 62 MeV our result with BGP density agrees nicely with experimental data over the whole angular range. Earlier, Hassan et al. [8], Spasova et al. [10] and very recently, Sharma and Haider [11] have analyzed $(d\sigma/d\Omega)$ data for $p-^{9,11}\text{He}$ elastic scattering at these energies. These authors employed either density reliant M3Y and KH effective NN interaction potential within the optical model framework or hybrid model of the microscopic optical potential or using the BHF have calculated the optical potential. Though, these researchers obtained fair success nevertheless it is well known

that optical model based analyses involve at least four to six adjustable parameters to reproduce the experimental data. Further, it is well acknowledged that the shell model or else mean field based calculations cannot be employed directly in neutron rich halo nuclei due to small binding energy of the last nucleons (neutrons). The result obtained by these calculations is, therefore, not essentially produce the precise account of lightly bound halo nuclei. Here, it is worth to mention that in our approach, no free/adjustable parameter has been used to analyze the elastic scattering data. Each parameter of NN scattering amplitude is experimentally known and our phenomenological BGP density contains no free parameter.

Table III presents the results of total reaction cross sections σ_R for ^{11}Li . For comparison, corresponding σ_R obtained indicated in past have also been displayed in the same Table. The σ_R for $p-^{11}\text{Li}$ probably has not yet been experimentally studied. Our calculated values of σ_R at energies are quite large as compared to estimated values in [10], [11].

TABLE III
THE CALCULATED REACTION CROSS SECTIONS FOR $p-^{11}\text{Li}$ AT ENERGIES 62,68.4 AND 75 MeV

| Energy | 62 MeV | | 68.4 MeV | | 75 MeV | |
|------------------------|------------------|-----|------------------|-----|------------------|-----|
| Authors | σ_R in mb | | σ_R in mb | | σ_R in mb | |
| Present Calculation | 514.0 | | 455.5 | | 429.0 | |
| Sharma and Haider [11] | 330 | 415 | 379 | 426 | 295 | 360 |
| K Spasova et al [10] | 457 | 462 | 122 | 154 | 232.6 | |

For comparison, the corresponding cross sections obtained reported earlier have also been shown.

V. CONCLUSION

The elastic proton-nucleus scattering has demonstrated to be an effective technique for finding detailed and complete statistics on the size and radial shape of nuclei called halo nuclei. In this paper, $p-^9\text{Li}$ and $p-^{11}\text{Li}$ elastic scattering differential cross sections in the energy range 60~75 MeV have been studied by means of Coulomb modified Glauber scattering formalism [12]. By applying the semi-phenomenological BGP [13] nuclear density for loosely bound ^{11}Li , the estimated matter rms radius is found to be 3.446 fm which is quite large as compared to so known experimental value 3.12 fm by Tanihata et al. [2]. It is to be noted that in most of phenomenological density model used to reproduce the $p-^{11}\text{Li}$ differential elastic scattering cross sections, calculated matter radius varies with minimum 2.964 fm [20] to a maximum 3.55 fm [5], [6]. Interestingly, quite similar pattern has also been seen for tail (halo) radius, however, not large variations are found in the value of rms core radius obtained by earlier studies reported in this work.

We also have found that our results with phenomenological BGP [13] model density reproduces $p-^9\text{Li}$ and $p-^{11}\text{Li}$ experimental data quite nicely as compared to GG or GO densities [5] at all energies under consideration. Here, it is worth commenting that, in our approach, no free/adjustable parameter has been used to analyze the elastic scattering data of $p-^{9,11}\text{Li}$ at energy range 60 75 MeV/nucleon as against the

well-known optical model based analyses that involves at least four to six adjustable parameters to reproduce the experimental data. Our calculated total reaction cross sections σ_R for p- ^{11}Li elastic scattering at these energies are quite large as compared to estimated values in [10], [11] though so far no experimental studies has been performed to measure it.

REFERENCES

- [1] I. Tanihata, et al. "Measurements of interaction cross sections and nuclear radii in the light p-shell region," *Phys. Rev. Lett.*, vol. 55, pp. 2676-79, Dec.1985.
- [2] I. Tanihata et al. "Determination of the density distribution and the correlation of halo neutrons in ^{11}Li ," *Phys. Lett. B*, vol. 287, pp. 307-311, Jan.1992.
- [3] G. D. Alkhozov, S. L. Belostotsky, A. A. Vorobyov, "Scattering of 1 GeV protons on nuclei," *Phys. Reports*, vol. 42, pp. 89-144 June 1978.
- [4] P. Egelhofaf, "Probing the halo structure of exotic nuclei by direct reactions with radioactive beams," *Nucl. Phys. A*, vol. 722, pp. C254-60, July 2003.
- [5] A. V. Dobrovolsky et al. "Study of the nuclear matter distribution in neutron-rich Li isotopes," *Nucl. Phys. A*, vol. 766, pp. 1-24, Feb. 2006.
- [6] J. S. Al-Khalili and J. A. Tostevin, "Matter radii of light halo nuclei," *Phys. Rev. Lett.*, vol. 76, pp. 3903-06, May 1996.
- [7] C.B. Moon et al. "Measurements of $^{11}\text{Li} + p$ and $^9\text{Li} + p$ elastic scatterings at 60 MeV," *Phys. Lett. B*, vol. 297, pp. 39-43, Dec. 1992.
- [8] M. Y. M. Hassan, M. Y. H. Farag, H. E. H. Esmael and H. M. Maridi, "Microscopic model analysis of $^{11}\text{Li} + p$ elastic scattering at 62, 68.4, and 75 MeV/nucleon," *Phys. Rev. C*, vol. 79, pp. 014612, Jan. 2009.
- [9] V.K. Lukyanov et al. "Microscopic analysis of ^{11}Li elastic scattering on protons and breakup processes within the $^9\text{Li} + 2n$ cluster model," *Phys. Rev. C*, vol. 88, pp. 034612, Sept. 2013.
- [10] K Spasovaet al. "Microscopic analysis of ^{11}Li elastic scattering on protons and breakup processes within $^9\text{Li} + 2n$ cluster model," *Journal of Physics: Conference Series* 2014, vol. 1, p. 012031. IOP Publishing
- [11] Manjari Sharma and W. Haider, "Study of $^{11}\text{Li} + p$ elastic scattering using BHF formalism with three body force," *J. Phys. G: Nucl. and Particle Phys.*, vol. 45, pp. 045102, March 2018.
- [12] S. K. Charagi, S. K Gupta, "Coulomb-modified Glauber model description of heavy-ion reaction cross sections," *Phys. Rev. C*, vol. 41, pp. 1610-18 April 1990.
- [13] A. Bhagwat, Y. K. Gambhir and S. H. Patil, "Nuclear densities of Li isotopes," *J. Phys. G: Nucl. Particle Phys.*, vol. 27, B1-B7, Feb. 2001.
- [14] R. J. Glauber, in *Lecture on Theoretical Physics vol. 1*, ed. by W.E. Brittin, L.C. Dunham (Interscience, New York, 1959), p. 315
- [15] B. Abu-Ibrahim, W. Horiuchi, A. Kohama and Y. Suzuki, "Reaction cross sections of carbon isotopes incident on a proton," *Phys. Rev. C*, vol. 77, pp. 034607, March 2008.
- [16] M.A. Alvi, "Study of Different Forms of Density Distributions in Proton-Nucleus Total Reaction Cross Section and the Effect of Phase in NN Amplitude," *Braz. J. Phys.*, vol 44, pp. 55-63, Jan. 2014
- [17] I. Ahmad, M. A. Abdulmomen, L. A. Al-Khattabi, "Alpha-nucleus total reaction cross section in the rigid projectile model using microscopic N- α amplitude," *Int. J. Modern Phys. E*, vol. 10, pp. 43-53, Feb. 2001.
- [18] Y. K. Gambhir, S. H. Patil, "Some characteristics of nuclear densities," *Z. Physik A Atomic Nuclei*, vol. 324, pp. 9-13, March 1986.
- [19] G. Baur and S. Typel, "Direct reactions with exotic nuclei, nuclear structure and astrophysics," *Prog. Part. Nucl. Phys.*, vol. 59(1), pp. 122-30, July 2007
- [20] J. S. Karataglidis, P. J. Dortmans, K. Amos, and C. Bennhold, "Alternative evaluations of halos in nuclei," *Phys. Rev. C*, vol. 61, pp. 024319, Jan. 2000
- [21] Syed Rafi, A. Bhagwat, W. Haider, and Y. K. Gambhir, "Brueckner-Hartree-Fock-based optical potential for proton- $^{4,6,8}\text{He}$ and proton- $^{6,7,9,11}\text{Li}$ scattering," *Phys. Rev. C*, vol. 86, pp. 034612, Sept. 2012.